energies

MDPI

Article

Experimental Study of Mixed Gas Hydrates from Gas Feed Containing CH_4, CO_2 and N_2: Phase Equilibrium in the Presence of Excess Water and Gas Exchange

Ludovic Nicolas Legoix [1,2,*], Livio Ruffine [2,*], Christian Deusner [1] and Matthias Haeckel [1]

[1] GEOMAR, Helmholtz Centre for Ocean Research Kiel, Wischhofstr. 1-3, D-24148 Kiel, Germany; cdeusner@geomar.de (C.D.); mhaeckel@geomar.de (M.H.)

[2] Institut Français de Recherche pour l'Exploitation de la Mer (IFREMER), Centre de Bretagne, Département Ressources Physiques et Ecosystèmes de Fond de Mer, Unité des Géosciences Marines, 29280 Plouzané, France

* Correspondence: llegoix@geomar.de (L.N.L.); Livio.Ruffine@ifremer.fr (L.R.)

Received: 8 July 2018; Accepted: 30 July 2018; Published: 31 July 2018

Abstract: This article presents gas hydrate experimental measurements for mixtures containing methane (CH_4), carbon dioxide (CO_2) and nitrogen (N_2) with the aim to better understand the impact of water (H_2O) on the phase equilibrium. Some of these phase equilibrium experiments were carried out with a very high water-to-gas ratio that shifts the gas hydrate dissociation points to higher pressures. This is due to the significantly different solubilities of the different guest molecules in liquid H_2O. A second experiment focused on CH_4-CO_2 exchange between the hydrate and the vapor phases at moderate pressures. The results show a high retention of CO_2 in the gas hydrate phase with small pressure variations within the first hours. However, for our system containing 10.2 g of H_2O full conversion of the CH_4 hydrate grains to CO_2 hydrate is estimated to require 40 days. This delay is attributed to the shrinking core effect, where initially an outer layer of CO_2-rich hydrate is formed that effectively slows down the further gas exchange between the vapor phase and the inner core of the CH_4-rich hydrate grain.

Keywords: gas hydrates; CH_4; CO_2; N_2; high-pressure experiments; phase equilibrium; gas exchange

1. Introduction

Clathrate hydrates are crystallographic structures made up of cage-forming water molecules containing small guest molecules (e.g., Sloan and Koh [1]). In the environment, these are typically natural gas compounds and as a consequence gas hydrates are encountered below the permafrost in polar regions, and in marine sediments of all active and passive continental margins (e.g., Claypool and Kvenvolden [2], Kvenvolden [3], Pinero et al. [4]). While CH_4 is the most notorious gas molecule being the dominant natural gas, larger natural gas compounds with specific steric hindrance like ethane, propane and isobutane can also be enclathrated into the water lattice (e.g., Kida et al. [5], Lu et al. [6], Bourry et al. [7]). Amongst the notable physicochemical properties of gas hydrates are their high selectivity in enclathrating guest molecules and the high storage capacity of those gases (e.g., Gudmundsson et al. [8], Sloan [9], Sloan and Koh [1], Eslamimanesh et al. [10]).

In the first part of the presented work, mixed gas hydrates formed from CO_2, N_2 and CH_4 gases are studied, providing thermodynamic data on systems relevant to CO_2 storage in the gas hydrate phase, potentially coupled to CH_4 production from natural CH_4 hydrates. In the marine environment depleted oil and gas reservoirs, saline aquifers or deep-sea sediments are foreseen as geological units

for the storage of the anthropogenic CO_2 emitted at industrial point sources [11]. In this context, the formation of CO_2 hydrates has been discussed as natural seal that may form under suitable ambient pressure and temperature (*p*-*T*) conditions at the interface between the stored liquid CO_2 and the ocean water [12] or sedimentary porewater [13]. Meanwhile, interest in using natural CH_4 hydrates as an energy resource is growing and several production field tests have been conducted in recent years. Both processes, sub-surface carbon storage and gas hydrate exploitation, can be combined. For example, the exposure of CH_4 hydrates to a CO_2:N_2 (23:77 mol/mol) gas mixture has been studied in laboratory experiments by Park et al. [14], and this mixture was also used in the Ignik Sikumi CH_4 production field test below the Alaskan permafrost [15,16]. N_2 acts as a carrier gas and its admixture to CO_2 avoids technical and safety problems involved in using a dense liquid CO_2 phase. This mixture is also representative for flue gas emitted by power plants: exhaust gases produced by oxy-fuel and partial oxidation processes exceeds 40 mol-% CO_2, but flue gas from combustion power plants or industrial furnaces usually contains only 4–27 mol-% CO_2 [17], mixed with trace of other gases, such as (O_2, H_2S, NO_x), while the dominant component is N_2 [18].

CO_2-N_2-CH_4 gas streams injected in water can lead to the occurrence of a large variety of phase equilibria depending on the *p*-*T* conditions and the molar composition of the system, such as vapor-liquid equilibrium (VLE), Hydrate-Vapor-Liquid Equilibrium (HVLE), Hydrate-Liquid-Liquid-Vapor Equilibrium (HLLVE).

Accordingly, it is clearly important to investigate phase equilibrium thermodynamics of gas mixtures made of CH_4, CO_2 and N_2 at *p*-*T* conditions relevant to gas hydrate formation. The N_2-CH_4 system was already reviewed and studied by Duan and Hu [19] and the VLE on the binary CO_2-N_2 has already been investigated and recently reviewed with addition of new data [20,21]. Moreover, CO_2 is more soluble in an aqueous phase than CH_4 and N_2 under ambient temperature conditions, which shows the importance to consider the water phase proportion in the system.

In our work, a set of experiments provides HVLE thermodynamic data of the CH_4-CO_2-H_2O, CO_2-N_2-H_2O and CH_4-CO_2-N_2-H_2O systems. While the CO_2-CH_4-H_2O system has been investigated and summarized by Kastanidis et al. [22], data collected for the two other systems are presented here in Tables 1 and 2. The collected data are in accordance and the injected water proportion from other works is always considered as low, with no impact on gas composition due to dissolution differences between gases. Sun et al. [23] flushed the gas several times at equilibrium with liquid H_2O before starting the gas hydrate formation, in order to have the vapor phase at the dissolution point similar to the gas feed. Thus, in this work the feed gas is systematically considered as the gas composition at the gas hydrate dissociation point, as in the work from other authors (Tables 1 and 2). The second part of our work presents experimental results of gas exchange between the vapor and the gas hydrate phase, with CH_4 and CO_2 gases. Several laboratory studies of gas exchange within a gas hydrate phase were performed, especially for CH_4-CO_2 exchange using different fluid phases, porous media and additives, reviewed by Deusner et al. [24] and by Komatsu et al. [25]. Here, the aim was to investigate the phenomena that occurs when a CH_4 hydrate is coexisting with a CO_2 vapor phase outside its initial stability zone, taking in consideration the slow evolution of gas exchange due to solid-state diffusion.

Table 1. Overview of Hydrate-Vapor-Liquid equilibrium (HVLE) experimental data for the ternary system CO_2-N_2-H_2O.

Reference	*T*/K *p*/MPa	CO_2 Mole Fraction	Number of Data Points
[26]	273.1–280.2 1.22–3.09	$z^*_{CO_2}$ = 0.9099–0.9652	9
[27]	273.4–281.9 1.986–9.550	$z^*_{CO_2}$ = 0.20–0.75 $y^*_{CO_2}$ = 0.1620–0.7189	15
[28,29]	272.85–284.25 1.565–24.12	$z^*_{CO_2}$ = 0.0663–0.9659	28

Table 1. *Cont.*

Reference	*T*/K *p*/MPa	CO_2 Mole Fraction	Number of Data Points
[30]	273.7 7.7	$z^*_{CO_2}$ = 0.169 $y^*_{CO_2}$ = 0.139	1
[31]	275.3–283.1 1.6–22.4	$z^*_{CO_2}$ = 0.21–0.80 $y^*_{CO_2}$ = 0.162–0.787	24
[32]	273.4–281.1 5.30–6.60	$y^*_{CO_2}$ = 0.16–0.59	16
[33]	276.88–285.41 5.0–20.0	$z^*_{CO_2}$ = 0.841–0.906	16
[34]	273.6–281.7 2.032–17.628	y_{CO_2} = 0.127–0.747	35
[35]	278.1–285.3 3.24–29.92	$z^*_{CO_2}$ = 0.271–0.812	9
[36]	275.0–281.1 8.23–24.51	$z^*_{CO_2}$ = 0.1–0.2	17
[37]	273.4–278.4 5.28–17.53	$z^*_{CO_2}$ = 0.101–0.251	17
[38]	275.75–284.45 5–20	$z^*_{CO_2}$ = 0.26–0.36	10
[39]	270.5–278.3	$z^*_{CO_2}$= 0.01–0.47	9
This work	276.06–280.97 9.762–20.583	$z^*_{CO_2}$ = 0.2317	4

Table 2. Overview of HVLE experimental data for the quaternary system CH_4-CO_2-N_2-H_2O.

Reference	*T*/K *p*/MPa	CH_4 Mole Fraction	CO_2 Mole Fraction	N_2 Mole Fraction	Number of Data Points
[40]	276.85–293.41 3.454–23.979	$z^*_{CH_4}$ = 0.9497	$z^*_{CO_2}$ = 0.05	$z^*_{N_2}$ = 0.0003	6
[41]	ca. 274–282 ca. 2–5	$z^*_{CH_4}$ = 0.41–0.55	$z^*_{CO_2}$ = 0.29–0.40	$z^*_{N_2}$ = 0.05–0.30	26
[42]	284.50–289.34 8.75–11.23	$z^*_{CH_4}$ = 0.8989	$z^*_{CO_2}$ = 0.05	$z^*_{N_2}$ = 0.0511	6
[43]	279.6–293.0 4.81–30.66	$z^*_{CH_4}$ = 0.5–0.9	$z^*_{CO_2}$ = 0.02–0.1	$z^*_{N_2}$ = 0.08–0.4	30
[23]	274.9–283.9 2.29–14.97	$y^*_{CH_4}$ = 0.203–0.826	$y^*_{CO_2}$ = 0.052–0.604	$y^*_{N_2}$ = 0.05–0.577	45
[44]	276.2–286.3 2.59–8.84	$z^*_{CH_4}$ = 0.4995–0.7005	$z^*_{CO_2}$ = 0.1998–0.4503	$z^*_{N_2}$ = 0.0490–0.1093	34
This work	282.46–288.62 9.679–15.645	$z^*_{CH_4}$ = 0.46–0.941	$z^*_{CO_2}$ = 0.015–0.14	$z^*_{N_2}$ = 0.044–0.379	5

2. Experiments

2.1. Experimental Setups

The experimental apparatus consists of a compact high-pressure cell (Figure 1, designed by the Service Ingénierie et Instrumentation Marine (SIIM), IFREMER, Plouzané, France) made of Titanium TA6V, operating at temperatures between 263 and 373 K, and for pressure up to 30 MPa. A three-port valve allows connecting the cell to a pressure transducer (±0.01 MPa) Serie 23 SY (Keller, Winterthur, Switzerland), together with either a vacuum pump or a fluid injection system. To quickly establish equilibrium conditions, a magnetic stirrer is mixing the solution. The cell is immerged in a thermal bath regulated by a temperature controller ECO Silver RE 12 (Lauda, Lauda-Königshofen, Germany) and monitored by a K-Type thermocouple (±0.4 K). A high-pressure liquid metering pump Optos (Eldex Laboratories Inc., Napa, CA, USA) is used to inject precise amounts of water into the cell. The total volume of the cell, including the magnetic stirrer and the connected pressure transducer, is 51.8 (±0.1) mL. This volume was determined by three injections of 2-propanol pressurized up

to 9.8 MPa at a fixed temperature of 313.35 K following the procedure described by Ruffine and Trusler [45]. The mass of the injected liquid was measured by weighing; dividing by the fluid density applying the model of Zuniga and Galicia [46] gave the volume of the cell.

The apparatus employed for the gas replacement experiment is a high-pressure variable-volume view cell, with a volume set to 26.9 mL. A detailed description of this apparatus can be found elsewhere [47,48].

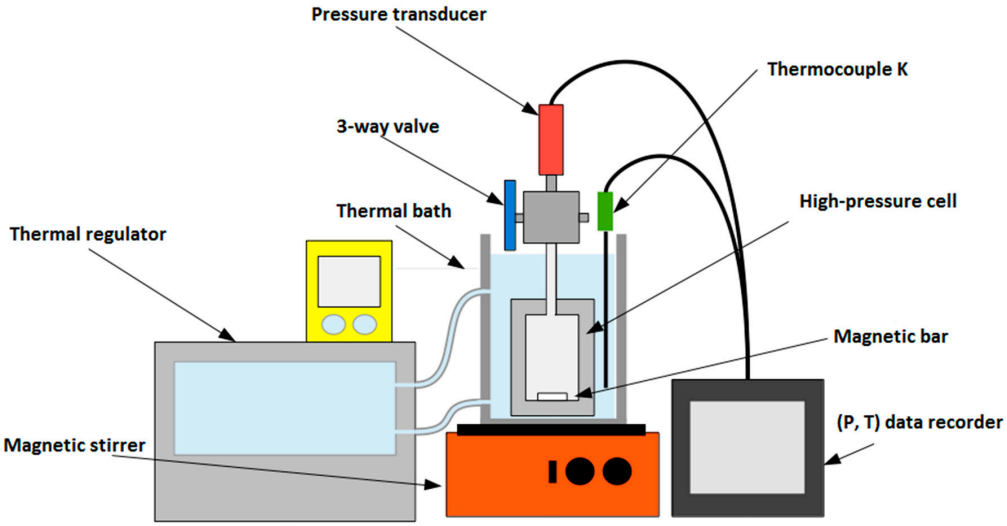

Figure 1. Sketch of the high-pressure cell designed to collect thermodynamic data of mixed gas hydrates.

2.2. Materials

All gases were supplied by L'Air Liquide. When used as single gas, CH_4, CO_2 and N_2 had a claimed purity of 0.99995 by mole content. Two binary gas mixtures, CO_2-N_2 and CO_2-CH_4, were used in this study with a reported composition of 0.2317 ($\pm$0.46) and 0.8996 ($\pm$0.10) mol-% of CO_2, respectively. Deionized water with a resistivity of 18.2 MΩ cm was degassed by boiling before using it.

2.3. Experimental Procedures

For the measurements of dissociation points, the gas composition was analyzed with a gas chromatograph GC-MS 7890A-5975C (Agilent Technology, Santa Clara, CA, USA) before injecting the deionized water. A Flame Ionization Detector (FID) was used to quantify CH_4, whereas N_2 and CO_2 were measured with a Thermal Conductivity Detector (TCD). When needed, a gas booster DLE 5-15 (Maximator GmbH, Nordhausen, Germany) was used to inject at higher pressures than gas bottle pressure. Then water was injected with the metering pump, the temperature was decreased and the stirrer was switched on to form gas hydrates. The pressure drop indicates the formation of gas hydrates. A heating procedure [49], with step-wise temperature increments of 0.5 K every 2 h was used to monitor the *p-T* of dissociation of mixed gas hydrates. This experimental setup and procedure employed to measure phase equilibrium with the Titanium pressure cell was validated by measuring HVLE data of pure CH_4 and pure H_2O. A *p-T* dissociation point of (9.459 MPa, 285.79 K) is measured, which is in good agreement with the average value of (9.441 MPa, 285.74 K) from other experiments [50–53].

The gas exchange experiment was carried out in the high-pressure view cell. It consisted in the formation of pure CH_4 hydrates with 10.2 g of H_2O, followed by a depressurization under self-preservation temperature at 265.7 K. When the pressure reached almost 1 bar, the gaseous CO_2 is pressurized into the cell, in order to replace CH_4 molecules in the gas hydrate lattices. The temperature is set to 277.8 K for the rest of the experiment and the evolution of the pressure and of the vapor phase composition were monitored over time.

3. Results and Discussion

3.1. Phase Equilibrium of Mixed Gas Hydrates

A series of experiments were carried out to measure HVLE for the ternary mixtures N_2-CO_2-H_2O and CH_4-CO_2-H_2O, and the quaternary mixture CH_4-CO_2-N_2-H_2O (Table 3). At 270 K, a minimum of 57 mol-% of CO_2 (more for higher temperature) is required to form a CO_2-rich liquid phase from a CO_2-N_2 mixture [54]. For the CO_2-CH_4 mixture at 273.15 K, clearly more than 60 mol-% of CO_2 is required to form a CO_2-rich liquid phase [48,55]. Thus, no CO_2-rich liquid phase is possible to form since the CO_2 composition of our gas mixtures is always low enough and the temperatures high enough.

Table 3. HVLE data for the systems CO_2-N_2-H_2O, CH_4-CO_2-H_2O and CH_4-CO_2-N_2-H_2O.

T/K	*p* /Mpa Experiment	*p*/MPa CSMGem (Deviation %) [1]	$z^*_{N_2}$	$z^*_{CO_2}$	$z^*_{CH_4}$	H_2O:Gas Feed Molar Ratio	H_2O Saturation vol.%
276.06	9.762	11.165 (14.4)	0.7683	0.2317	0	19.45	58.3
277.63	12.584	14.504 (15.3)	0.7683	0.2317	0	21.52	66.8
279.09	16.373	18.539 (13.2)	0.7683	0.2317	0	24.32	74.9
280.97	20.583	23.873 (16.0)	0.7683	0.2317	0	24.25	78.2
280.92	3.410	3.5798 (5.0)	0	0.8996	0.1004	44.66	83.2
282.61	4.291	4.3982 (2.5)	0	0.8996	0.1004	37.46	83.2
284.97	6.206	6.3211 (1.9)	0	0.8996	0.1004	42.47	91.9
282.46	9.679	No convergence	0.40	0.14	0.46	5.31	41.5
283.37	10.964	10.419 (−5.0)	0.38	0.14	0.48	6.32	39.4
284.11	13.102	10.901 (−16.8)	0.34	0.12	0.54	5.49	40.3
285.70	15.055	13.860 (−7.9)	0.37	0.13	0.50	4.67	39.6
288.62	15.645	14.068 (−10.1)	0.044	0.015	0.941	3.90	38.4

Moreover, a very recent study based on Raman spectroscopic measurements highlighted that a CO_2-N_2 gas mixture needs to contain a minimum of 98 mol-% N_2 to coexist with a structure II gas hydrate [39]. Thus, all gas hydrates are considered as structure I gas hydrate when the CO_2-N_2-CH_4 gas mixture was used. In our work, the water proportion was very high (Table 3), thus in the vapor phase at HVLE, the composition of the more soluble gas compound must decrease (but was not measured here). In Figure 2 our data are plotted together with some data of Kang et al. [29] and Lee et al. [36] who measured phase equilibria with gas feed compositions close to ours. Their data with 10 mol-% of CO_2 are also plotted, showing that a decrease of the CO_2:N_2 ratio in the system leads to an increase of the dissociation pressure. For a given N_2-CO_2 gas feed and a given temperature, the equilibrium pressure increases with water content compared to a system with a lower water-to-gas ratio (Figure 2). This implies that the gas hydrate stability domain for a flue gas injected into a large water-rich system will likely be shifted to higher pressures. This pressure shift is also noticeable if the feed gas is richer in CO_2 (84.1–90.6 mol-%) with a high H_2O water content [33]. This finding is in agreement with Beltran et al. [56] who highlighted the importance of correctly defining either the initial gas feed and water amount or the composition of the vapor when determining the gas hydrate point of dissociation.

In the following paragraphs, the CSMGem program [1] has been used to predict the composition of the vapor and hydrate phases at the dissociation point. CSMGem is a thermodynamic model that computes the *p*-*T* conditions of dissociation of gas hydrates and its corresponding phase compositions for a given global composition including H_2O and different gases. With a CO_2-N_2 gas feed, at 276.06 K and 11.165 MPa (Table 3) the CSMGem program [1] gives a composition of 49.1 mol-% of CO_2 in the gas hydrate phase, and 10.7 mol-% in the vapor (23.17 mol-% in the feed gas). However, if the water content in a system with the same initial gas composition is increased, the CO_2 content in the vapor phase decreases due to its high solubility in liquid water at ambient temperature conditions. The solubility of different gases, i.e., distribution between the vapor and aqueous phase, affects the gas hydrate composition. Generally, most of studies investigate gas hydrate equilibria by measuring the

vapor phase composition at equilibrium or using only very small amounts of water so that the vapor composition stays almost unchanged during the experiments. At a defined temperature, increasing the content of N_2 in the vapor phase increases the composition of the gas hydrate in N_2 and increases its pressure of dissociation.

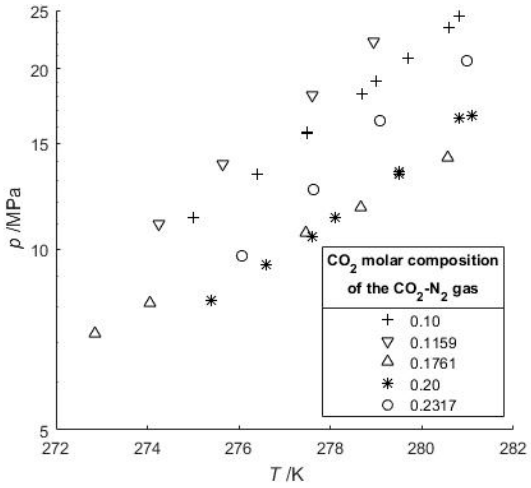

Figure 2. Hydrate-Vapor-Liquid Equilibrium (HVLE) data of the CO_2-N_2-H_2O system. Our study provides data for 23.17 mol-% CO_2 and high H_2O content. The datasets at low and high pressure correspond to 20 and 10 mol-% of CO_2 in the gas phase [36], and 17.61 and 11.59 mol-% of CO_2 [29], respectively.

Our three HVLE data points at gas hydrate dissociation conditions with 10 mol-% CH_4 (Table 3) are complementary to the HLLE (i.e., Hydrate-Liquid-Liquid Equilibrium) data presented in a previous study with the same gas feed composition under higher pressures, when no vapor is present [48].

For a CO_2-CH_4 gas feed with 89.96 mol-% CO_2, at 280.92 K and 3.5798 MPa (Table 3) the CSMGem program gives a composition of 73.9 mol-% of CO_2 in the gas hydrate phase, and 63.1 mol-% in the vapor phase. However, for a negligible amount of water the calculated pressure does not change significantly (3.3049 MPa) because the HVLE *p*-*T* curves of CO_2 and CH_4 are relatively close to each other compared to the curves of CO_2 and N_2. Finally, a series of HVLE data measured with a lower water content and a CO_2-N_2-CH_4 gas feed are in accordance with recent literature data (Figure 3).

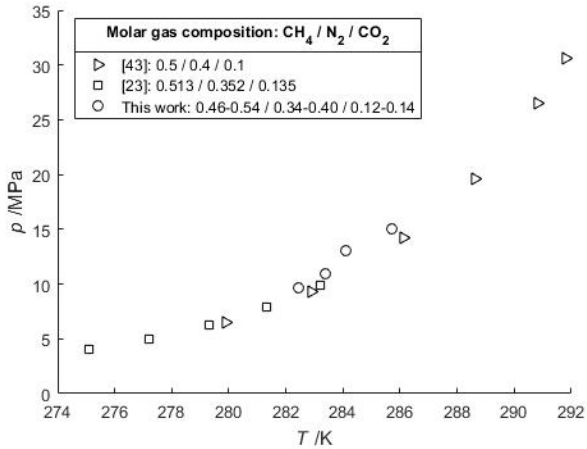

Figure 3. Comparison of HVLE data of typical pretreated CO_2-N_2 flue gas compositions that are diluted by CH_4 gas (50 mol-%) in natural gas hydrate settings.

3.2. CH_4-CO_2 Exchange between a Vapor Phase and a Bulk Gas Hydrate Phase

The objective of this experiment was to study the gas exchange mechanism between an initial bulk CH_4 hydrate phase after exposure to a surrounding CO_2 vapor phase (Figure 4). In the experiment CH_4 hydrate is formed from pure CH_4 and pure H_2O, and subsequently the gas feed is changed to CO_2. The temperature is held constant during the reaction, while pressure and vapor composition are monitored. After injecting CO_2 the pressure is kept below the stability pressure of pure CH_4 hydrate, but still above the stability pressure of pure CO_2 hydrate during the entire gas hydrate exchange experiment. After 6 days the vapor phase contains 60.3 mol-% of CH_4, while the pressure has approached 2.90 MPa at a temperature of 277.7 K. For these input parameters, CSMGem [1] predicts a gas hydrate containing 43.2 mol-% of CH_4 that has a dissociation pressure of 2.79 MPa. However, after 6 days when the experiment was stopped, the curves of pressure and vapor phase composition still show a very gentle slope (Figure 5) indicating that complete thermodynamic equilibrium has not yet been achieved and the exchange reaction is still slowly progressing. The following paragraph discusses the possible processes occurring in the batch experiment.

Figure 4. Top panel: Visual observation of the evolution of the different phases during gas hydrate crystallization (from left to right: directly after water injection; after stirrer has been set to 400 rpm; 1 min after the gas hydrate formation incipient; 48 min after the gas hydrate formation incipient). **Bottom** panel: Visual state of the system during the gas exchange process (from left to right: t = 0 h; t = 1.47 h; t = 18.90 h; t = 89.73 h; t = 118.90 h; t = 145.73 h).

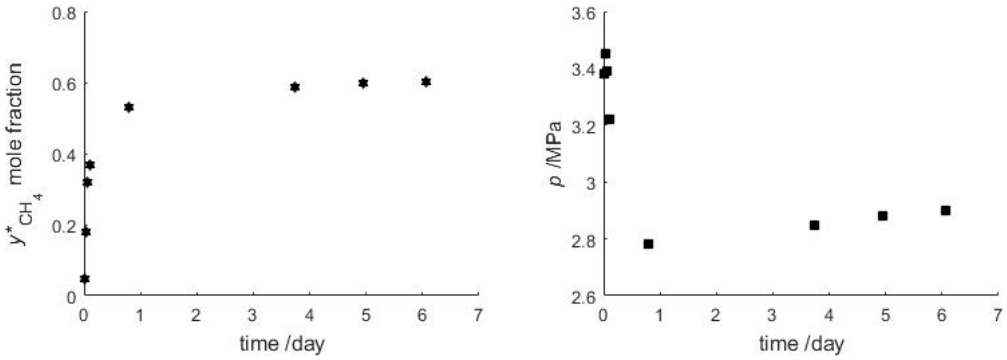

Figure 5. Evolution of the composition of the vapor phase (**Left**) and evolution of the pressure (**Right**) during the replacement of CH_4 by CO_2. See Table A1 (Appendix A) for the list of measured values.

The observed change in gas composition and pressure evolution indicate that the experiment can be split in two parts (Figure 5). At the beginning the CH_4 vapor content increases very quickly to 40 mol-%, while the overall pressure drops by 0.6 MPa, indicating CH_4 hydrate dissociation being

decoupled from CO_2 hydrate formation. In addition, the observed overall pressure drop can only result from CO_2 consumption by hydrate formation with excess water in the cell. In the second phase the pressure in the cell is slowly increasing again, complemented by a parallel further, gentle CH_4 increase in the vapor phase, indicating that a coupled gas exchange of CH_4 by CO_2 in the hydrate phase becomes the dominant process. This direct gas hydrate conversion has been described previously by the shrinking-core process [57].

Here, CO_2 replaces the CH_4 in the hydrate grain forming an outer CO_2-rich hydrate shell around an inner CH_4 hydrate core. Consequently, gas exchange is controlled by the percolation of gas molecules through the CO_2-rich hydrate shell, i.e., CH_4 is transported to the vapor phase surrounding the hydrate grains and CO_2 is transported from the outside to the inner CH_4 hydrate core. Thus, the kinetics of the coupled hydrate conversion is generally slow and depends on the size of the CH_4 hydrate grains.

In the following mass balance we attempt to discriminate the three processes, CH_4 hydrate dissociation, CO_2-rich hydrate formation from excess water and shrinking-core hydrate conversion, from each other. The total amount of CO_2 in the batch cell, initially exists only in the vapor phase, i.e., at 2.69 MPa and 265.7 K a gas volume of 16.7 cm^3 is equivalent to 2.69×10^{-2} mol of CO_2. The initial mass of H_2O of 10.2 g was measured with a scale. Then, the initial CH_4 amount in the system is 9.94×10^{-2} mol, considering 1 atm of CH_4 that remained in the vapor phase plus the CH_4 bound in gas hydrate formed from 10.2 g of H_2O, assuming a constant hydration number of 5.75 (i.e., $h_{H_2O} = 0.852$). The aim is to constrain the proportion of the CO_2 hydrate that was effectively formed with the corresponding excess H_2O, and to extrapolate the end time of the gas exchange between the CH_4 hydrate and the CO_2-rich vapor phase. For the rate of the gas exchange, here is considered a linear increase of CH_4 coming from the gas hydrate phase, enriching the vapor phase. This linear increase for our system is measured from the slope of the last two data points of our experiment (Figure 5):

$$y^*_{CH_4}\,[\text{mole fraction}] = 2.236 \times 10^{-4} \times t\,[/\text{hour}] + 0.570$$

$$p\,[/\text{MPa}] = 7.454 \times 10^{-4} \times t\,[/\text{hour}] + 2.791$$

The total amounts of each component (CH_4, CO_2, H_2O) in the system and the observed average temperature of 277.8 K are used as inputs for the CSMGem program that returns the corresponding composition of phases at thermodynamic equilibrium and the pressure of the mixed gas hydrate dissociation (HVLE). The resulting $y^*_{CH_4}$ and $h^*_{CH_4}$ (i.e., molar fraction of CH_4 within gas hydrate compared to CO_2) together with the phase fraction calculated at the end of the gas exchange, give a new value of the total amount of CH_4. For each iteration, the total fraction of each component is changed leading each time to a lower proportion of initial CH_4 hydrate formed. The calculation is finished when the mass balance is reached.

The result shows that 86.2% of H_2O was consumed initially to form the pure CH_4 hydrate, i.e., 13.8% remained as liquid excess water in the cell. The gas exchange between CH_4 and CO_2 in the hydrate is finished supposedly within 39.7 days, resulting in a mixed gas hydrate containing 62.7 mol-% of CH_4 ($h^*_{CH_4}$) and a vapor phase containing 78.4 mol-% of CH_4 ($y^*_{CH_4}$). This means that 1.4 g of H_2O would not have been bound in CH_4 hydrate at the beginning (i.e., being excess water), which is in agreement with the pressure decrease initially observed. This pressure decrease is due to the formation of CO_2-rich hydrate consuming 0.7 g of excess water (dissolution of CO_2 in liquid H_2O would require using 7.7 g of H_2O to achieve the same pressure drop).

4. Conclusions

A series of phase equilibrium (HVLE) experiments with different gas mixtures of CH_4-CO_2, CO_2-N_2 and CH_4-CO_2-N_2 were conducted. Compared to previous work in the literature the data shows that the disparity of solubility in the aqueous phase between gases strongly affects the dissociation

pressure of mixed gas hydrates at a given temperature, especially for flue-gas type containing CO_2 and N_2. Since CO_2-N_2 gas mixtures are considered for a CH_4 production from gas hydrate reservoirs, or the storage of a flue gas in a natural setup (below the permafrost or within the sediments on continental margins), the water saturation level of the sediment will then systematically affect the stability of the gas hydrate formed from CO_2-N_2-(CH_4) mixtures. These gas hydrates could have a thermodynamic stability affected by the complex evolution of the environment during and after the injection. Thus, the CO_2-N_2-containing mixed hydrate formed in the vicinity of the well may become unstable, if surrounding formation water flows towards the well.

The gas exchange experiment performed outside pure CH_4 hydrate stability pressure confirms that several processes are competing during the gas hydrate exchange: direct CO_2-CH_4 exchange within the initial CH_4 hydrate, dissociation of the initial CH_4 hydrate, and formation of CO_2-rich hydrate with excess water. Complete conversion of CH_4 hydrate to CO_2 hydrate will typically take several weeks to months, depending on the CH_4 hydrate grain size.

As a perspective, there is a need of thermodynamic and kinetic data of phase evolutions (i.e., gas hydrate growth and dissociation) of the CH_4-CO_2-N_2-H_2O system in presence of gas hydrates. Moreover, further studies on hydrate kinetics need to be done to evaluate better the competition between gas hydrate dissociation and direct gas exchange in a closed system, and during a depressurization process.

Author Contributions: Conceptualization, L.N.L., L.R. and C.D.; Writing—original draft, L.N.L., L.R. and M.H.

Funding: This research was supported by the SUGAR project, funded by the German Ministry of Research (grant number 03G0856A), and the 'Fluid migration within sedimentary environments', a research focus of the Geochemical Laboratory (LCG-GM-REM-IFREMER).

Conflicts of Interest: The authors declare no conflict of interest.

Abbreviations

Term	Symbol	Unit
Vapor phase composition of molecule *i*	y_i	mole fraction
Vapor phase composition of molecule *i* without H_2O	y^*_i	mole fraction
Gas hydrate composition of molecule *i* (i.e., hydration number for H_2O)	h_i	mole fraction
Gas hydrate composition of guest molecule *i*	h^*_i	mole fraction
Global composition of molecule *i* in the system	z_i	mole fraction
Global composition of molecule *i* in the system without H_2O	z^*_i	mole fraction

Appendix A

Table A1. Evolution of the gas phase with a CO_2-CH_4 gas exchange on an initial CH_4 hydrate.

Time after Gas Replacement/h	*T*/K	*p*/MPa	$y^*_{CH_4}$ Mole Fraction
0.53	277.0	3.38	0.049
0.97	277.8	3.45	0.178
1.47	277.8	3.39	0.318
2.65	277.8	3.22	0.368
18.90	277.7	2.78	0.530
89.73	277.7	2.85	0.586
118.90	277.8	2.88	0.597
145.73	277.7	2.90	0.603

References

1. Sloan, E.D., Jr.; Koh, C.A. *Clathrate Hydrates of Natural Gases*; CRC Press: Boca Raton, FL, USA, 2007.

2. Claypool, G.E.; Kvenvolden, K.A. Methane and other hydrocarbon gases in marine sediment. *Annu. Rev. Earth Planet. Sci.* **1983**, *11*, 299–327. [CrossRef]
3. Kvenvolden, K.A. Methane hydrate—A major reservoir of carbon in the shallow geosphere? *Chem. Geol.* **1988**, *71*, 41–51. [CrossRef]
4. Pinero, E.; Marquardt, M.; Hensen, C.; Haeckel, M.; Wallmann, K. Estimation of the global inventory of methane hydrates in marine sediments using transfer functions. *Biogeosciences* **2013**, *10*, 959. [CrossRef]
5. Kida, M.; Khlystov, O.; Zemskaya, T.; Takahashi, N.; Minami, H.; Sakagami, H. Coexistence of structure I and II gas hydrates in Lake Baikal suggesting gas sources from microbial and thermogenic origin. *Geophys. Res. Lett.* **2006**, *33*, L24603. [CrossRef]
6. Lu, H.; Seo, Y.T.; Lee, J.W.; Moudrakovski, I.; Ripmeester, J.A.; Chapman, N.R.; Coffin, R.B.; Gardner, G.; Pohlman, J. Complex gas hydrate from the Cascadia margin. *Nature* **2007**, *445*, 303. [CrossRef] [PubMed]
7. Bourry, C.; Chazallon, B.; Charlou, J.L.; Donval, J.P.; Ruffine, L.; Henry, P.; Geli, L.; Cagatay, M.N.; Moreau, M. Free gas and gas hydrates from the Sea of Marmara, Turkey: Chemical and structural characterization. *Chem. Geol.* **2009**, *264*, 197–206. [CrossRef]
8. Gudmundsson, J.S.; Parlaktuna, M.; Khokhar, A.A. Storing natural-gas a frozen hydrate. *SPE Prod. Facil.* **1994**, *9*, 69–73. [CrossRef]
9. Sloan, E.D. Fundamental principles and applications of natural gas hydrates. *Nature* **2003**, *426*, 353–359. [CrossRef] [PubMed]
10. Eslamimanesh, A.; Mohammadi, A.H.; Richon, D.; Naidoo, P.; Ramjugernath, D. Application of gas hydrate formation in separation processes: A review of experimental studies. *J. Chem. Thermodyn.* **2012**, *46*, 62–71. [CrossRef]
11. Lackner, K.S. A guide to CO_2 sequestration. *Science* **2003**, *300*, 1677–1678. [CrossRef] [PubMed]
12. Ohgaki, K.; Makihara, Y.; Takano, K. Formation of CO_2 hydrate in pure and sea waters. *J. Chem. Eng. Jpn.* **1993**, *26*, 558–564. [CrossRef]
13. House, K.Z.; Schrag, D.P.; Harvey, C.F.; Lackner, K.S. Permanent carbon dioxide storage in deep-sea sediments. *Proc. Natl. Acad. Sci. USA* **2006**, *103*, 12291–12295. [CrossRef] [PubMed]
14. Park, Y.; Kim, D.Y.; Lee, J.W.; Huh, D.G.; Park, K.P.; Lee, J.; Lee, H. Sequestering carbon dioxide into complex structures of naturally occurring gas hydrates. *Proc. Natl. Acad. Sci. USA* **2006**, *103*, 12690–12694. [CrossRef] [PubMed]
15. Schoderbek, D.; Farrell, H.; Howard, J.; Raterman, K.; Silpngarmlert, S.; Martin, K.; Smith, B.; Klein, P. *ConocoPhillips Gas Hydrate Production Test*; U.S. Department of Energy: Washington, DC, USA, 2013.
16. Boswell, R.; Schoderbek, D.; Collett, T.S.; Ohtsuki, S.; White, M.; Anderson, B.J. The Ignik Sikumi Field Experiment, Alaska North Slope: Design, Operations, and Implications for CO_2–CH_4 Exchange in Gas Hydrate Reservoirs. *Energy Fuels* **2016**, *31*, 140–153. [CrossRef]
17. Car, A.; Stropnik, C.; Yave, W.; Peinemann, K.V. Pebax®/polyethylene glycol blend thin film composite membranes for CO_2 separation: Performance with mixed gases. *Sep. Purif. Technol.* **2008**, *62*, 110–117. [CrossRef]
18. Linga, P.; Adeyemo, A.; Englezos, P. Medium-pressure clathrate hydrate/membrane hybrid process for postcombustion capture of carbon dioxide. *Environ. Sci. Technol.* **2007**, *42*, 315–320. [CrossRef]
19. Duan, Z.; Hu, J. A new cubic equation of state and its applications to the modeling of vapor-liquid equilibria and volumetric properties of natural fluids. *Geochim. Cosmochim. Acta* **2004**, *68*, 2997–3009. [CrossRef]
20. Fandino, O.; Trusler, J.M.; Vega-Maza, D. Phase behavior of (CO_2 + H_2) and (CO_2 + N_2) at temperatures between (218.15 and 303.15) K at pressures up to 15 MPa. *Int. J. Greenh. Gas Control.* **2015**, *36*, 78–92. [CrossRef]
21. Westman, S.F.; Jacob Stang, H.G.; Lovseth, S.W.; Austegard, A.; Snustad, I.; Storset, S.O.; Ertesvag, I.S. Vapor-liquid equilibrium data for the carbon dioxide and nitrogen (CO_2 + N_2) system at the temperatures 223, 270, 298 and 303 K and pressures up to 18 MPa. *Fluid Phase Equilib.* **2016**, *409*, 207–241. [CrossRef]
22. Kastanidis, P.; Romanos, G.E.; Stubos, A.K.; Economou, I.G.; Tsimpanogiannis, I.N. Two-and three-phase equilibrium experimental measurements for the ternary CH_4 + CO_2 + H_2O mixture. *Fluid Phase Equilib.* **2017**, *451*, 96–105. [CrossRef]
23. Sun, Y.H.; Li, S.L.; Zhang, G.B.; Guo, W.; Zhu, Y.H. Hydrate phase equilibrium of CH_4 + N_2 + CO_2 gas mixtures and cage occupancy behaviors. *Ind. Eng. Chem. Res.* **2017**, *56*, 8133–8142. [CrossRef]

24. Deusner, C.; Bigalke, N.; Kossel, E.; Haeckel, M. Methane Production from Gas Hydrate Deposits through Injection of Supercritical CO_2. *Energies* **2012**, *5*, 2112–2140. [CrossRef]
25. Komatsu, H.; Ota, M.; Smith, R.L., Jr.; Inomata, H. Review of CO_2-CH_4 clathrate hydrate replacement reaction laboratories studies-properties and kinetics. *J. Taiwan Inst. Chem. Eng.* **2013**, *44*, 517–537. [CrossRef]
26. Fan, S.S.; Guo, T.M. Hydrate formation of CO_2-rich binary and quaternary gas mixtures in aqueous sodium chloride solutions. *J. Chem. Eng. Data* **1999**, *44*, 829–832. [CrossRef]
27. Olsen, M.B.; Majumdar, A.; Bishnoi, P.R. Experimental Studies on Hydrate Equilibrium-Carbon Dioxide and Its Systems. *Int. J. Soc. Mater. Eng. Res.* **1999**, *7*, 17–23. [CrossRef]
28. Seo, Y.T.; Kang, S.P.; Lee, H.; Lee, C.S.; Sung, W.M. Hydrate phase equilibria for gas mixtures containing carbon dioxide: A proof-of-concept to carbon dioxide recovery from multicomponent gas stream. *Korean J. Chem. Eng.* **2000**, *17*, 659–667. [CrossRef]
29. Kang, S.P.; Lee, H.; Lee, C.S.; Sung, W.M. Hydrate phase equilibria of the guest mixtures containing CO_2, N_2 and tetrahydrofuran. *Fluid Phase Equilib.* **2001**, *185*, 101–109. [CrossRef]
30. Linga, P.; Kumar, R.; Englezos, P. Gas hydrate formation from hydrogen/carbon dioxide and nitrogen/carbon dioxide gas mixtures. *Chem. Eng. Sci.* **2007**, *62*, 4268–4276. [CrossRef]
31. Bruusgaard, H.; Beltrán, J.G.; Servio, P. Vapor− liquid water− hydrate equilibrium data for the system N_2 + CO_2 + H_2O. *J. Chem. Eng. Data* **2008**, *53*, 2594–2597. [CrossRef]
32. Herri, J.M.; Bouchemoua, A.; Kwaterski, M.; Fezoua, A.; Ouabbas, Y.; Cameirão, A. Gas hydrate equilibria for CO_2–N_2 and CO_2–CH_4 gas mixtures—Experimental studies and thermodynamic modelling. *Fluid Phase Equilib.* **2011**, *301*, 171–190. [CrossRef]
33. Kim, S.H.; Do Seo, M.; Kang, J.W.; Lee, C.S. Hydrate-containing phase equilibria for mixed guests of carbon dioxide and nitrogen. *Fluid Phase Equilib.* **2011**, *306*, 229–233. [CrossRef]
34. Belandria, V.; Eslamimanesh, A.; Mohammadi, A.H.; Richon, D. Gas hydrate formation in carbon dioxide+ nitrogen+ water system: Compositional analysis of equilibrium phases. *Ind. Eng. Chem. Res.* **2011**, *50*, 4722–4730. [CrossRef]
35. Sfaxi, I.B.A.; Belandria, V.; Mohammadi, A.H.; Lugo, R.; Richon, D. Phase equilibria of CO_2 + N_2 and CO_2 + CH_4 clathrate hydrates: Experimental measurements and thermodynamic modelling. *Chem. Eng. Sci.* **2012**, *84*, 602–611. [CrossRef]
36. Lee, Y.; Lee, S.; Lee, J.; Seo, Y. Structure identification and dissociation enthalpy measurements of the CO_2+N_2 hydrates for their application to CO_2 capture and storage. *Chem. Eng. J.* **2014**, *246*, 20–26. [CrossRef]
37. Sun, S.C.; Liu, C.L.; Meng, Q.G. Hydrate phase equilibrium of binary guest-mixtures containing CO_2 and N_2 in various systems. *J. Chem. Thermodyn.* **2015**, *84*, 1–6. [CrossRef]
38. Sadeq, D.; Iglauer, S.; Lebedev, M.; Smith, C.; Barifcani, A. Experimental determination of hydrate phase equilibrium for different gas mixtures containing methane, carbon dioxide and nitrogen with motor current measurements. *J. Nat. Gas Sci. Eng.* **2017**, *38*, 59–73. [CrossRef]
39. Chazallon, B.; Pirim, C. Selectivity and CO_2 capture efficiency in CO_2-N_2 clathrate hydrates investigated by in-situ Raman spectroscopy. *Chem. Eng. J.* **2018**, *342*, 171–183. [CrossRef]
40. Nixdorf, J.; Oellrich, L.R. Experimental determination of hydrate equilibrium conditions for pure gases, binary and ternary mixtures and natural gases. *Fluid Phase Equilib.* **1997**, *139*, 325–333. [CrossRef]
41. Lee, H.H.; Ahn, S.H.; Nam, B.U.; Kim, B.S.; Lee, G.W.; Moon, D.; Shin, H.J.; Han, K.W.; Yoon, J.H. Thermodynamic stability, spectroscopic identification, and gas storage capacity of CO_2–CH_4–N_2 mixture gas hydrates: implications for landfill gas hydrates. *Environ. Sci. Technol.* **2012**, *46*, 4184–4190. [CrossRef] [PubMed]
42. Kakati, H.; Mandal, A.; Laik, S. Phase stability and kinetics of CH_4 + CO_2 + N_2 hydrates in synthetic seawater and aqueous electrolyte solutions of NaCl and $CaCl_2$. *J. Chem. Eng. Data* **2015**, *60*, 1835–1843. [CrossRef]
43. Lim, D.; Ro, H.; Seo, Y.; Seo, Y.J.; Lee, J.Y.; Kim, S.J.; Lee, J.; Lee, H. Thermodynamic stability and guest distribution of CH_4/N_2/CO_2 mixed hydrates for methane hydrate production using N_2/CO_2 injection. *J. Chem. Thermodyn.* **2017**, *106*, 16–21. [CrossRef]
44. Zang, X.; Liang, D. Phase Equilibrium Data for the Hydrates of Synthesized Ternary CH_4/CO_2/N_2 Biogas Mixtures. *J. Chem Eng. Data* **2017**, *63*, 97–201. [CrossRef]
45. Ruffine, L.; Trusler, J. Phase behaviour of mixed-gas hydrate systems containing carbon dioxide. *J. Chem. Thermodyn.* **2010**, *42*, 605–611. [CrossRef]

46. Zuniga-Moreno, A.; Galicia-Luna, L.A. Densities of 1-Propanol and 2-Propanol via Vibrating Tube Densimeter from 313 to 363 K up to 25 MPa. *J. Chem. Eng. Data* **2002**, *47*, 155–160. [CrossRef]
47. Ruffine, L.; Donval, J.P.; Charlou, J.L.; Cremière, A.; Zehnder, B.H. Experimental study of gas hydrate formation and destabilisation using a novel high-pressure apparatus. *Mar. Pet. Geol.* **2010**, *27*, 1157–1165. [CrossRef]
48. Legoix, L.N.; Ruffine, L.; Donval, J.P.; Haeckel, M. Phase Equilibria of the CH_4-CO_2 Binary and the CH_4-CO_2-H_2O Ternary Mixtures in the Presence of a CO_2-Rich Liquid Phase. *Energies* **2017**, *10*, 2034. [CrossRef]
49. Tohidi, B.; Burgass, R.W.; Danesh, A.; Østergaard, K.K.; Todd, A.C. Improving the accuracy of gas hydrate dissociation point measurements. *Ann. N. Y. Acad. Sci.* **2000**, *912*, 924–931. [CrossRef]
50. McLeod, H.O., Jr.; Campbell, J.M. Natural gas hydrates at pressures to 10,000 psia. *J. Pet. Technol.* **1961**, *13*.
51. Adisasmito, S.; Frank, R.J.; Sloan, E.D., Jr. Hydrates of carbon dioxide and methane mixtures. *J. Chem. Eng. Data* **1991**, *36*, 68–71. [CrossRef]
52. Yang, S.O.; Yang, I.M.; Kim, Y.S.; Lee, C.S. Measurement and prediction of phase equilibria for water + CO_2 in hydrate forming conditions. *Fluid Phase Equilib.* **2000**, *175*, 75–89. [CrossRef]
53. Mohammadi, A.H.; Anderson, R.; Tohidi, B. Carbon monoxide clathrate hydrates: Equilibrium data and thermodynamic modeling. *AIChE J.* **2005**, *51*, 2825–2833. [CrossRef]
54. Somait, F.A.; Kidnay, A.J. Liquid-vapor equilibriums at 270.00 K for systems containing nitrogen, methane, and carbon dioxide. *J. Chem. Eng. Data* **1978**, *23*, 301–304. [CrossRef]
55. Nasir, Q.; Sabil, K.M.; Lau, K.K. Measurement of isothermal (vapor+ liquid) equilibria, (VLE) for binary (CH_4 + CO_2) from T = (240.35 to 293.15) K and CO_2 rich synthetic natural gas systems from T = (248.15 to 279.15) K. *J. Nat. Gas Sci. Eng.* **2015**, *27*, 158–167. [CrossRef]
56. Beltran, J.G.; Bruusgaard, H.; Servio, P. Gas hydrate phase equilibria measurement techniques and phase rule considerations. *J. Chem. Thermodyn.* **2012**, *44*, 1–4. [CrossRef]
57. Falenty, A.; Qin, J.; Salamantin, A.N.; Yang, L.; Kuhs, W.F. Fluid composition and kinetics of the in situ replacement in CH_4-CO_2 hydrate system. *J. Phys. Chem. C* **2016**, *120*, 27159–27172. [CrossRef]